

Martin Sladký <sup>1</sup>, Martin Machač <sup>2</sup>, Jan Papuga <sup>2</sup> & Ivo Jebáček <sup>1</sup>

<sup>1</sup>Faculty of Mechanical Engineering, Brno University of Technology, Brno, Czech Republic <sup>2</sup>Faculty of Mechanical Engineering, Czech Technical University in Prague, Prague, Czech Republic

#### **Abstract**

This contribution addresses the fatigue life prediction of thin-walled welded joints, which play indispensable roles in various aircraft structures. Following the recommendations of the International Institute of Welding (IIW), three main fatigue life prediction approaches (nominal stress, structural stress, and notch stress based predictions) are described. A comparative study is conducted on six types of specimens, providing insights from their fatigue testing and numerical determination of each stress type. The S-N curve slopes obtained from the evaluated data are consistent with general assumptions regarding thin-walled welded structures and a considerable split, dividing the evaluated data into two separate S-N curves, suggests the need for additional corrections to achieve more accurate fatigue life predictions.

**Keywords:** high cycle fatigue life prediction, thin-walled welded joints, nominal stress, structural stress, notch stress

#### 1. Introduction

Welded joints serve indispensable functions in connecting various aircraft components, playing a pivotal role not only in the design of engine mount but also in the construction of landing gear and parts of the flight control system. Due to the inherent nature of aircraft operations, these welded components are subjected to variable loading. However, welded joints exhibit a higher sensitivity, compared to the base material, to fatigue damage, resulting from this variability in loading, which makes them one of the primary locations for fatigue crack initiation. Therefore, an accurate assessment of welded joints' fatigue life is under these conditions inevitable.

However, as outlined in [1], predicting fatigue life in welded structures presents greater challenges and complexities compared to non-welded structures. The increased complexity is caused by a combination of internal factors, including inherent weld defects and deviations, residual stresses, and material heterogeneity. Additionally, this inherent complexity can be further deepened by external factors such as corrosion or elevated temperature.

Moreover, in addition to these aspects specific to welded joints, the relatively small thickness of typical aerospace components is also a significant factor influencing the resulting fatigue life. It has been observed and summarized for example in [2], that thin-walled structures exhibit higher slope exponents and knee points of the S-N curve relative to their thick-wall counterparts. As a result, fatigue life prediction of thin-walled joints based on knowledge obtained from tests of thick-walled samples leads to shorter predicted fatigue lives compared to the actual observations. This underestimation of real fatigue life results in heavier assemblies, which is undesirable in aerospace applications where weight reduction is crucial.

One of the most comprehensive sets of recommendations for predicting the fatigue life of welded joints is provided by the International Institute of Welding (IIW). The general guideline [3] encompasses recommendations for all three main stress-based prediction approaches. The first of these approaches, commonly described as the global approach, is based on the evaluation of nominal stress. The remaining two, described as local approaches, involve the evaluation of structural stress

and notch stress. Recognizing the heightened complexity associated with these two approaches, the IIW has also issued specific guidelines focused solely on the structural stress-based approach [4] and the notch stress-based approach [5]. Additionally, the general IIW guideline [3] outlines a prediction method based on the stress intensity factor and a basic fatigue crack propagation law. However, given its limitation to describing only the fatigue crack propagation phase, this approach is not included among the fatigue life prediction approaches utilized in this paper.

Other less standardized fatigue life prediction approaches predominantly rely on local parameters such as strain energy density, notch stress intensity factor, or various parameters derived from the theories of Linear Elastic Fracture Mechanics (LEFM) or Continuum Damage Mechanics (CDM). These approaches, although not yet incorporated into official technical norms or guidelines, offer valuable insights into fatigue life assessment. A comprehensive summary of these prediction approaches can be found in [6].

S-N curves, essential for fatigue life evaluation in all stress-based approaches, are defined in IIW guidelines by the FAT value, representing the maximum tolerable stress range for  $2 \cdot 10^6$  cycles, and their slope. According to IIW guideline [5] or for example article [7] the recommended slope of the S-N curve for thin-wall structures with a wall thickness of less than five millimeters under normal stress is 5, while for structures under shear stress, it is 7. The recommended FAT value varies depending on the specific evaluation approach and weld configuration.

This article aims to provide a concise overview of the three stress-based fatigue life prediction approaches mentioned above, with a specific focus on their application to thin-walled structures. Additionally, it aims to demonstrate the evaluation of fatigue life through a study involving six types of thin-walled welded specimens with diverse geometries and loading conditions, including two specimen configurations (I conf. and H conf.) tested directly at Czech Technical University in Prague. By analyzing the results obtained from this study, the article also seeks to offer insights that contribute to the understanding of fatigue life prediction in thin-walled welded structures.

# 2. Review of Employed Fatigue Life Prediction Approaches

### 2.1 Nominal stress based prediction

Nominal stress based prediction models represent the most traditional and straightforward approach to fatigue life prediction. This prediction method utilizes the so-called global approach to assessing the fatigue life of welded joints, where the nominal stress is defined as the stress value unaffected by stress concentrators (such as the weld joint, notch, etc.). Its determination relies on the basic mechanics of materials relationships, often without the need for adopting Finite Element Method (FEM) analysis.

Due to the complete disregard for stress concentration effects, these models have a significant limitation: they possess minimal ability to transfer results from one geometry to another. This necessitates the search for or creation of new specialized S-N curves for every new geometry, which is both time-consuming and expensive, especially when investigating atypical weld designs. Moreover, determining nominal stress in complex structures with intricate geometries may be ambiguous. Another drawback of nominal stress-based models, as described in [8], is their tendency to be overly conservative, particularly for high-quality welds compared to local approaches.

S-N curves for various structural details can be found in numerous guidelines and recommendations provided by leading standardization bodies, including the European Committee for Standardization (CEN) [9], the British Standards Institution (BSI) [10], the European Convention for Constructional Steelwork (ECCS) [11], the Deutscher Verband für Schweißen und verwandte Verfahren (DVS) [12], and the International Institute of Welding (IIW) [3].

The IIW guideline [3] also includes references to external documents, such as [13], that provide instructions for estimating recalculations between different geometries, particularly when dealing with minor changes such as variations in the thickness or dimensions of the selected detail. This process is essentially based on converting nominal stress to structural stress through the application of a stress concentration factor.

In this fatigue life prediction approach, the thickness effect is typically incorporated directly into the design S-N curve. For applications involving wall thicknesses greater than the standard value of 25 mm,

the IIW guideline [3] addresses the influence of plate thickness on fatigue strength by modifying the FAT value. This modification is determined using the following equation:

$$FAT_{eff} = FAT_{std} \cdot \left(\frac{t_{std}}{t_{eff}}\right)^n \tag{1}$$

where the thickness correction exponent n is dependent on the weld type and post-welded treatment, and the standard thickness  $t_{std}$  is set at  $25 \, \mathrm{mm}$ . The application of any type of benign thickness correction for thin-walled welded joints is not restricted, but according to IIW guideline [3], it must always be verified through a component test. For the subsequent fatigue life evaluation, the thickness correction was applied using this equation, which is well-established for thick components.

#### 2.2 Structural stress-based prediction

Structural stress refers to stress concentration at the notch solely caused by the geometrical detail, without considering the nonlinear concentration due to the presence of the notch. This concept is typically associated with finite element calculations nowadays. However, as outlined in [1], Haibach originally proposed this concept based on strain gauge measurements.

As described in more detail by [1], various definitions of structural stress exist, with the most conventional being the so-called hot-spot stress, named after the location of fatigue crack initiation. According to general IIW guideline [3], the hot-spot stress can be determined using linear extrapolation of the stress acting on the component's surface at distances of 0.4t and t from the weld toe, where t represents the wall thickness. This linear extrapolation is schematically illustrated in Figure 1. The Hot-Spot stress values can be obtained through either experimental means or numerical simulations. A simple equation for calculating hot-spot stress from the stress values at designated positions is:

$$\sigma_{hs} = 1.67 \sigma_{0.4t} - 0.67 \sigma_t \tag{2}$$

where  $\sigma_{hs}$  is required hot-spot stress,  $\sigma_{0.4t}$  is stress value obtained from the position 0.4t before weld toe and  $\sigma_t$  is is stress value obtained from the position t.

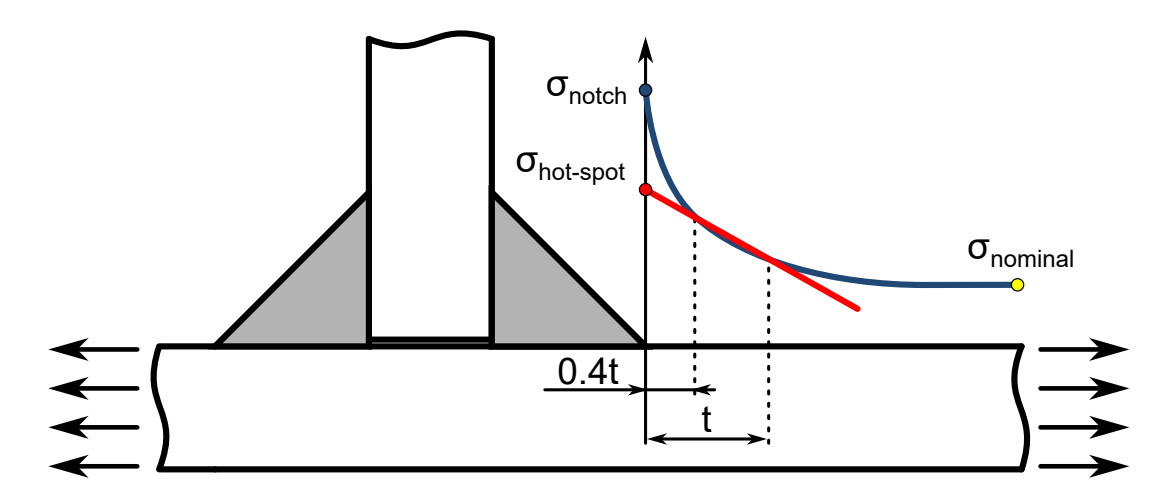


Figure 1 – Definitions of Stress Types Used for Predicting the Fatigue Life of Welded Joints.

In cases of steep stress gradients near the weld toe or when assessing stress from the sheet metal's side wall, this guideline employs quadratic extrapolation based on three points at distances of 0.4t, 0.9t, and 1.4t from the weld toe. Further, more detailed information on hot spot stress determination can be found in [4].

Less commonly used definitions of structural stress, often referred to as modified concepts of structural stress, are based on the linearization of stress in the component's cross-section. This linearization process involves virtually decomposing the acting stress  $\sigma$  into three separate components: membrane stresses  $\sigma_m$ , bending stresses  $\sigma_b$ , and equilibrium nonlinear peak stresses  $\sigma_{nl}$ , followed by the summation of membrane and bending stresses. This structural stress can only be determined

numerically, and, according to [8], its values, with slight deviations, generally align with the values of structural stress obtained by fitting stress data on the component's surface. Furthermore, this general concept has been further developed, with [14, 15] representing the most widely accepted modifications.

All IIW recommendations are focused primarily on determining hot-spot structural stress and as summarized by [1], the main advantage of this approach, compared to other local approaches, lies in its simplicity. The finite element mesh used to determine hot-spot structural stress can be significantly coarser than the mesh used for determining notch stress, strain energy density, or stress intensity factor, resulting in shorter calculation times. Additionally, it is much less sensitive to the influence of local imperfections, such as undercut or overlap, present in real geometry. However, a significant drawback of this approach is its inability to address weld root fatigue.

The thickness effect is addressed in the general IIW guideline [3] similarly to the nominal stress-based approach. This means that the FAT value for components thicker than 25 mm should be modified according to equation 1, and the application of any type of benign thickness correction for thin-walled welded joints must always be verified through a component test. For the subsequent fatigue life evaluation, the thickness correction was also established by equation 1.

# 2.3 Notch stress based prediction

The application of the notch stress-based prediction approach in welded joints relies on the assumption that the weld toe and weld root represent the same type of structural discontinuity as the notch. Consequently, in the assessment of fatigue life, the concept of linear-elastic effective notch stress, originally introduced by Neuber in [16], can be effectively applied. Neuber proposed that for sharp notches, the critical factor influencing high-cycle fatigue life is not the peak linear-elastic stress, but rather a slightly lower effective notch stress determined as the mean value at a characteristic material-dependent critical distance. This phenomenon is commonly referred to as the microstructural notch support effect.

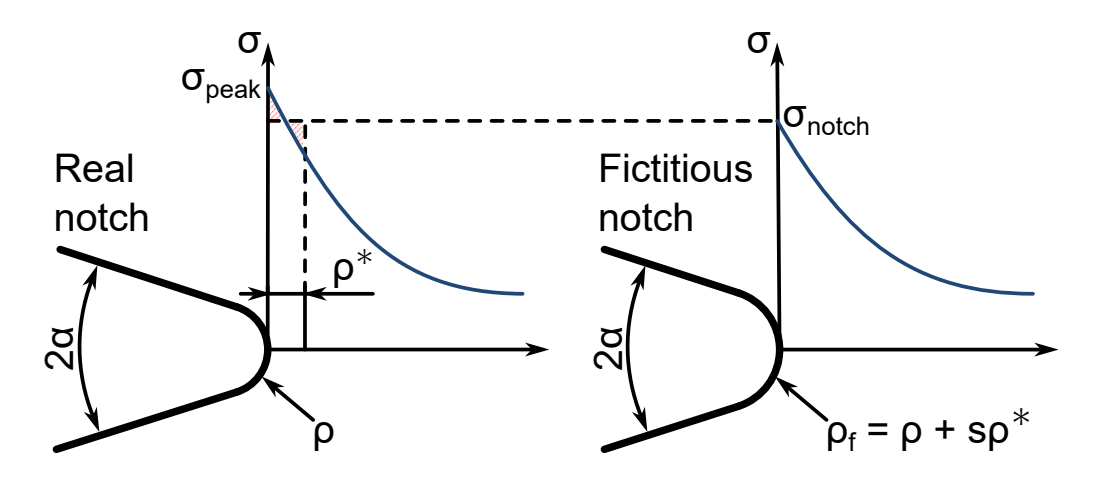


Figure 2 – Definition of Notch Stress by Introducing a Fictitious Notch Rounding.

This general concept was subsequently modified to facilitate the prediction of fatigue life in welded joints, especially when employing Finite Element Analysis. This modification is based on the introduction of the concept of a fictitious notch of a predefined radius. The underlying idea, illustrated schematically in Figure 2 and detailed in [17], is that by introducing a fictitious radius, the calculated linear-elastic peak stress at the notch root is reduced, making it equivalent to the effective notch stress value. As outlined in [1] the value of the fictitious radius can be determined using the following equation:

$$\rho_f = \rho + s\rho^* \tag{3}$$

which combines the actual notch radius  $\rho$  with a term  $s\rho^*$  accounting for Neuber's characteristic distance  $\rho^*$  and the multiaxial factor s. A recommended fictitious notch radius of one millimeter

is advised by IIW guidelines for components with a thickness of five millimeters or greater, made from structural steels and aluminum alloys. The application of this one-millimeter fictitious radius is consistently associated with only one FAT class: FAT225.

As discussed in [18], employing a one-millimeter fictitious radius in thin-walled structures with steep stress gradients often leads to nonconservative results, as the application of the one-millimeter fictitious radius gradually diminishes stress concentration in the notch. To address this issue, thin-walled welded structures commonly adopt a reference radius of  $r_{ref} = 0.05 \, \mathrm{mm}$ , initially introduced in connection with spot welds by [19]. This reference radius finds its roots in linear elastic fracture mechanics, where, in the case of spot welds, the resulting stress value serves as a rough approximation of the stress intensity factor. The IIW guideline [5] recommends the use of this reference radius for components thinner than five millimeters and associates it with only one FAT class: FAT630.

However, as summarized in [20], the reference radius approach, unlike the fictitious radius approach, does not correctly consider the microstructural support effect. Consequently, in the case of a reference radius based approach, the FAT value becomes dependent on the size of the notch opening angle. This discrepancy, as suggested in [21], leads to inaccuracies in describing the fatigue behavior of some weld configurations. According to [20], the general relationship between the FAT value and the reference radius, as a function of the notch opening angle size, can be roughly described by the following exponential equation:

$$FAT_{ref} = C \, r_{ref}^{-n} \tag{4}$$

where the exponent n is a function of the notch opening angle  $2\alpha$ , with n not exceeding 0.5 for a notch opening angle of  $2\alpha=0^{\circ}$ . Additionally, the constant C should approach the value of 225, referencing the FAT value for a fictitious radius of curvature  $\rho_f=1\,\mathrm{mm}$ . The table 1 summarizes FAT values derived from real fatigue tests, as described in [21], for various structural steels and aluminum alloys, considering actual fictitious and reference radii.

Table 1 – Recommended FAT values derived from real fatigue tests for structural steel and aluminum alloy in various failure locations, according to [21].

Structural Steel			
Location	$\rho_f = 1 \text{ mm}$	$r_{ref} = 0.3 \text{ mm}$	$r_{ref} = 0.05 \text{ mm}$
Root of Fillet Weld	FAT225	FAT340	FAT630
Toe of Fillet Weld	FAT225	FAT300	FAT500
Butt Weld Joint	FAT225	FAT250	FAT360
Aluminum Alloy			
Location	$\rho_f = 1 \text{ mm}$	$r_{ref} = 0.3 \text{ mm}$	$r_{ref} = 0.05 \text{ mm}$
Root of Fillet Weld	FAT71	FAT110	FAT200
Toe of Fillet Weld	FAT71	FAT95	FAT160
Butt Weld Joint	FAT71	FAT80	FAT112

The greatest advantage of the notch stress based fatigue life prediction approach lies in its generality. With just one S-N curve according to IIW recommendations or a few similar curves as per the latest scientific recommendations, it is possible to address fatigue failure at the weld toe or weld root in nearly every type of geometry. Additionally, the notch stress prediction approach stands out as the only stress-based method capable of directly addressing fatigue initiation originating at the notch root. Further details about the preparation of weld root geometry can be found in [22].

However, this generality comes at the cost of increased sensitivity to the influence of local imperfections, such as undercut or overlap, present in real-world geometries, and greater computational efforts. Particularly in the case of thin-walled welded joints with a reference radius of  $0.05\,\mathrm{mm}$ , finite element models can consist of several hundred thousand quadratic elements. Due to the significant computational effort required to obtain accurate notch stress, the DVS norm [12] introduces another fictitious radius of  $r_{ref}=0.3\,\mathrm{mm}$ , specifically recommended for medium-thickness components ranging from 2 to  $5\,\mathrm{mm}$  in thickness.

# 3. Experimental Setup and Numerical Stress Analysis

### 3.1 Description of Specimens and Conducted Experiments

A practical demonstration of fatigue life prediction for thin-walled welded joints is presented using six series of specimens. The first two series, comprising twelve specimens labeled as "I configuration" and fourteen as "H configuration", were Circular Hollow Section joints, described already in [23]. The next two series, consisting of three specimens labeled as "OPB configuration" and two as "IPB configuration", were Rectangular Hollow Section joints, described already in [24]. The last two series, comprising thirteen specimens labeled as "PS configuration" and eight as "PL configuration", were flat plates joined by a fillet weld, also described already in [24]. A graphical representation of each specimen, including the loading orientation, is shown in Figure 3. All specimens were tested in aswelded conditions.

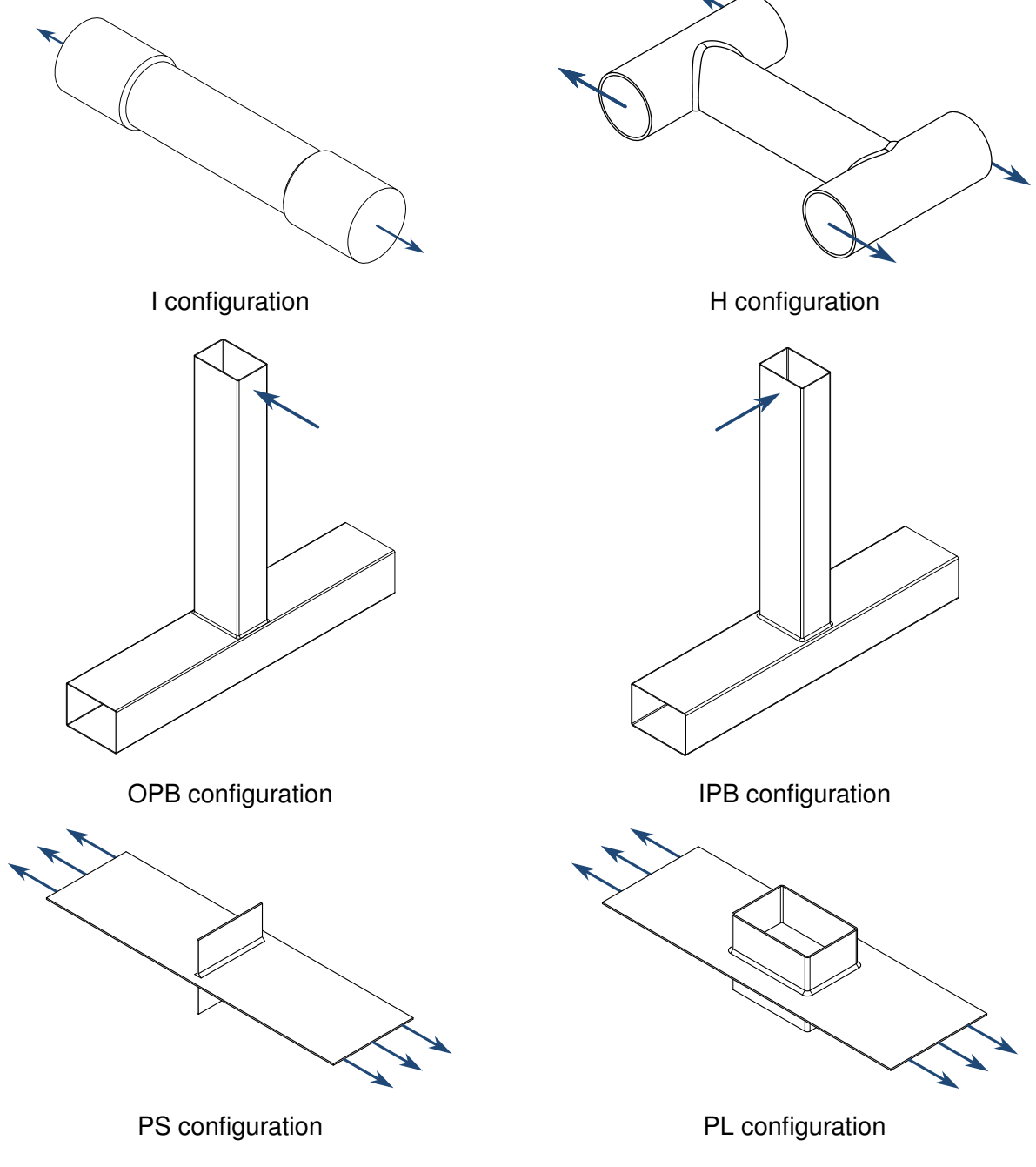


Figure 3 – Schematic Illustration of Evaluated Specimen Configurations with Loading Directions Indicated by Arrows.

The I configuration consists of a central tube and two circular bodies, with the central tube having a

wall thickness of  $1.24\,\mathrm{mm}$ , joined together by a load-carrying fillet weld with a size of  $z=2\,\mathrm{mm}$ . The specimen was loaded in the tension direction with a coefficient of load asymmetry R=0.1. Samples were made from structural steel AISI 4130-N with specification AMS6360. Radiographic checks for weld imperfections were conducted, revealing imperfections in three out of twelve specimens in this series. The first occurrence of a fatigue crack was observed mainly at the weld toe.

The H configuration consists of three perpendicular circular tubes with a central tube wall thickness of  $1.24\,\mathrm{mm}$  joined together by a load-carrying fillet weld with the size  $z=2\,\mathrm{mm}$ . The specimen was loaded by the pins placed in the outward (chord) tubes with a coefficient of load asymmetry R=0.1. Samples were made from structural steel AISI 4130-N with specification AMS6360. Radiographic checks for weld imperfections were conducted, revealing imperfections in eleven out of fourteen specimens in this series. However, the vast majority of defects were found far from the crack initiation site. The first occurrence of a fatigue crack was at the weld toe of the central (brace) tube near the saddle point.

The OPB configuration comprises two perpendicular rectangular tubes with a wall thickness of  $2\,\mathrm{mm}$  joined together by a load-carrying fillet weld with the size  $z=4\,\mathrm{mm}$ . The specimen was subjected to out-of-plane bending with a coefficient of load asymmetry  $R\approx 0.1$  and only a small preload. The specimens were fabricated from structural steel. Each test was concluded when a substantial amount of through-thickness cracking was observed. The first occurrence of a fatigue crack was observed at the weld toe of the tension side of the horizontal (chord) tube, located at the corner point of the welded joint.

The IPB configuration comprises two perpendicular rectangular tubes with a wall thickness of  $2\,\mathrm{mm}$  joined together by a load-carrying fillet weld with the size  $z=5\,\mathrm{mm}$ . The specimen was subjected to inplane bending with a coefficient of load asymmetry  $R\approx 0.1$  and only a small preload. The specimens were fabricated from structural steel. Each test was concluded when a substantial amount of throughthickness cracking was observed. The first occurrence of a fatigue crack was observed at the weld toe of the tension side of the horizontal (chord) tube, located at the corner point of the welded joint.

The PS configuration consists of three perpendicular plates with a wall thickness of  $2\,\mathrm{mm}$  joined by a non-load-carrying fillet weld with the size  $z=4\,\mathrm{mm}$ . The main plate was subjected to tension with a coefficient of load asymmetry R=0. For detailed information on the chemical composition of the steel used for this type of specimen, refer to [24]. Test termination was determined by the specimen's ultimate rupture. The first occurrence of a fatigue crack was observed at the weld toe of the main plate at the end of the perpendicular plates.

The PL configuration consists of a rectangular tube joined to a main plate by a non-load-carrying fillet weld with the size  $z=4\,\mathrm{mm}$ . Both parts of this specimen have a wall thickness of  $2\,\mathrm{mm}$ . The main plate was subjected to tension with a coefficient of load asymmetry R=0. For detailed information on the chemical composition of the steel used for this type of specimen, refer to [24]. Test termination was determined by the specimen's ultimate rupture. The first occurrence of a fatigue crack was observed at the weld toe of the main plate located at the corner of the welded joint.

The I configurations and the H configurations underwent testing using the Amsler HFP422 fatigue testing pulsator, with a load capacity of  $100\,\mathrm{kN}$  under force control. The H configurations were tested at a frequency ranging between 75 and  $90\,\mathrm{Hz}$ , while the I configurations were tested at a frequency of  $130\,\mathrm{Hz}$ . The OPB configurations and the IPB configurations were tested using a five-ton capacity servo-controlled hydraulic testing machine, operating under load control at a frequency of approximately  $3\,\mathrm{Hz}$ . Finally, the PS configurations and PL configurations were tested using the 100 kN Amsler Vibrophore fatigue testing pulsator, at a frequency of approximately  $240\,\mathrm{Hz}$ .

Further details on the I configuration and H configuration configurations, testing procedures, and results can be found in [23], while similar information for other specimen types is available in [24].

## 3.2 Evaluating Hot-Spot and Notch Stress

This subsection focuses solely on the numerical evaluation of hot-spot and notch stress, as nominal stress can be in almost every case determined using simple analytical equations. Except for the evaluation of hot-spot stress in I and H configurations, which was calculated using the Abaqus environment, all other calculations were performed in the Nastran solver.

Hot-spot stress and Notch stress values are defined as elastic stress values, thus there was no need to account for material nonlinearity. Except for the H configuration, where loading via pins inserted

into horizontal tubes introduced geometric nonlinearity due to changes in contact surfaces during loading, there is also no significant geometric nonlinearity. Therefore, the majority of tasks can be treated as linear-elastic problems.

All tested specimen types possess at least one plane of symmetry, which allows for a considerable reduction in computational time and resources. To enhance calculation accuracy while minimizing the number of elements, quadratic hexahedral and wedge elements were used to mesh all described tasks. A typical mesh used for the evaluation, incorporating only minor modifications specific to each specimen configuration, is shown in Figure 4.

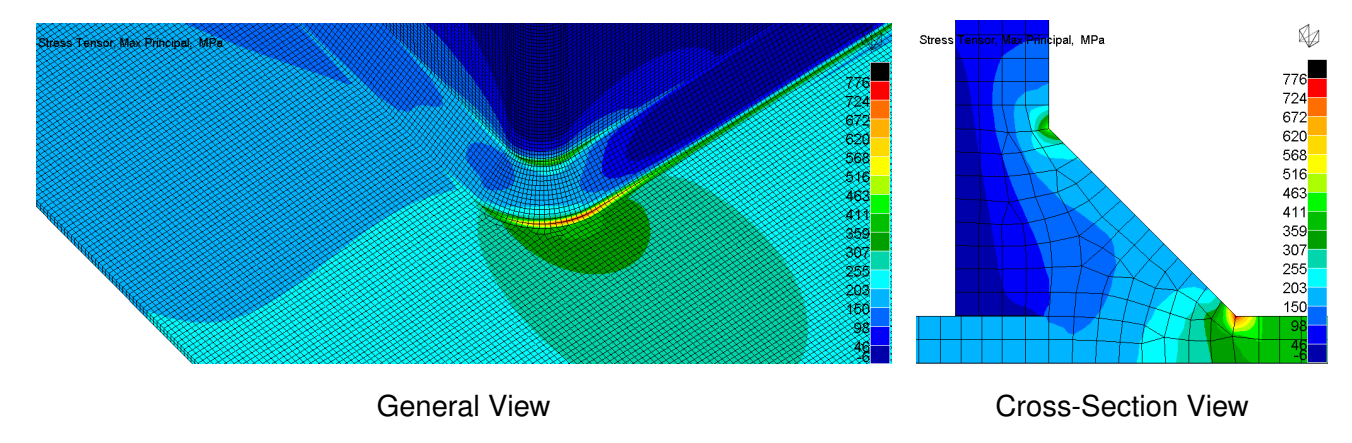


Figure 4 – Detailed Visualization of the Typical Mesh at the Critical Area and its Cross-Section.

However, despite these efforts, due to the requirements imposed by the IIW guidelines [3, 4, 5] for determining hot-spot and notch stresses, it is practically impossible to determine these stresses in complex geometries such as these without appropriately implementing a single submodel for hot-spot stress and two submodels for notch stress in the region of presumed fatigue crack initiation. Conclusions presented in [25] were used to minimize the numerical error caused by the implementation of each submodel.

The evaluation of hot-spot stress followed IIW recommendations for analyzing the weld toe on the plate surface, utilizing a linear extrapolation from points situated at distances 0.4t and t from the weld toe. The typical element edge size at the submodels ranged from  $0.15\,\mathrm{mm}$  for I configuration and H configuration, which have thinner walls, to  $0.2\,\mathrm{mm}$  for all other specimen configurations. According to IIW guidelines, the minimum mesh size for this case is set to 0.4t, with further mesh refinement left to the user's discretion. The mesh of the typical "hot-spot" submodel was created similarly to the mesh shown in Figure 4, with the element size scaled accordingly and the task volume reduced to only the critical area of each specimen configuration.

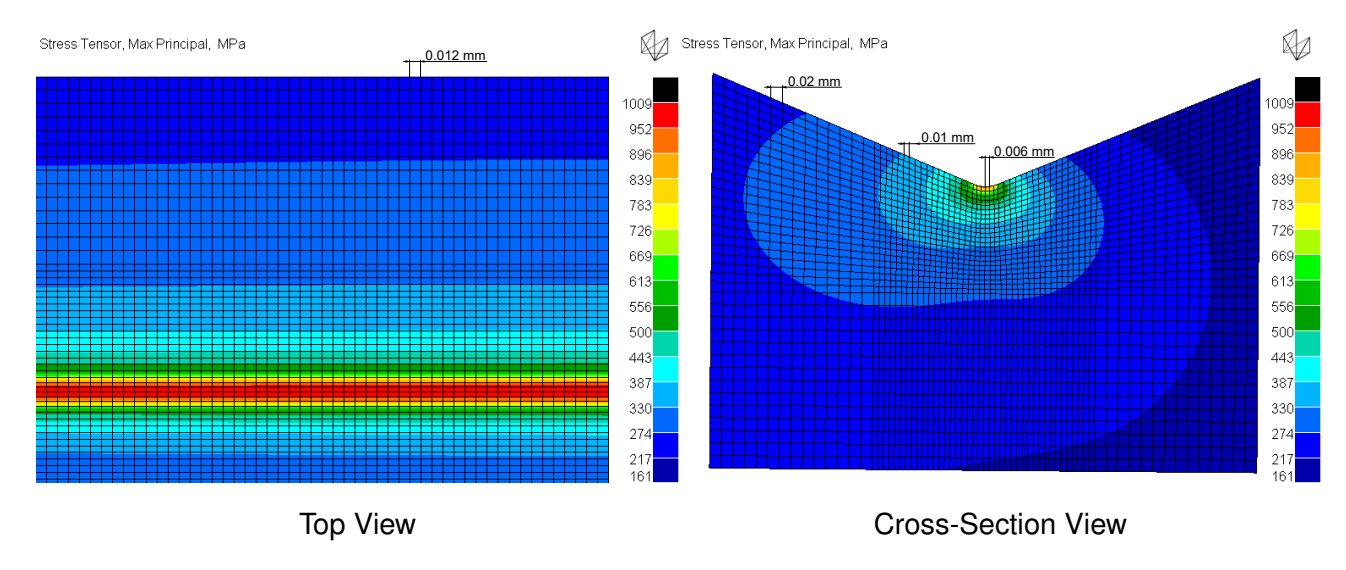


Figure 5 – Detailed Visualization of the Typical Mesh of the Final "Notch Stress" Submodel

The evaluation of notch stress, which is highly dependent on the size, type, and quality of the elements, was conducted using a second submodel created similarly for all types of specimens. The typical element edge size ranged from  $0.02\,\mathrm{mm}$  at the submodel boundaries to  $0.006\,\mathrm{mm}$  at the notch root. Figure 5 provides a detailed view of the mesh for the final "notch stress" submodel. According to IIW guidelines, the recommended minimum mesh size for second-order elements is  $0.012\,\mathrm{mm}$ , with further refinement left to the user's discretion. IIW guideline [5] specifies that notch stress calculated using this element type and size should not deviate from the actual value by more than approximately two percent. Comprehensive insights into meshing the notch root and selecting an appropriate mesh size are provided in [26].

## 4. Comparison of Prediction Approach Results

Base FAT classes were assigned to each specimen configuration according to IIW recommendations. To explore the possibilities of simple thickness effect correction, modified FAT values, calculated according to equation 1, were also included in the comparison. For the notch stress based evaluation, where the thickness effect is inherently included due to the nature of notch stress, and the assignment of a reference radius  $r_{ref} = 0.05 \, \mathrm{mm}$  ensures the accuracy of this evaluation even for structures with very thin walls, a comparison between FAT630 recommended by the IIW guideline [5] and FAT500 recommended for the weld toe of the fillet weld by [21] was demonstrated. All FAT values related to each specimen configuration are summarized in Tables 2 and 3 and all these values are related to the Maximum Principal Stress.

Table 2 – Base FAT values according to IIW recommendations.

Table 3 – Modified FAT values based on the thickness correction or failure position.

Approach:	Nominal	Hot-Spot	Notch
I conf.	FAT63	FAT90	FAT630
H conf.	FAT71	FAT100	FAT630
OPB conf.	FAT71	FAT100	FAT630
IPB conf.	FAT71	FAT100	FAT630
PS conf.	FAT80	FAT100	FAT630
PL conf.	FAT80	FAT100	FAT630

Approach:	Nominal	Hot-Spot	Notch
I conf.	FAT209	FAT299	FAT500
H conf.	FAT236	FAT333	FAT500
OPB conf.	FAT151	FAT213	FAT500
IPB conf.	FAT151	FAT213	FAT500
PS conf.	FAT171	FAT213	FAT500
PL conf.	FAT171	FAT213	FAT500

The assessment of fatigue life results generally involves statistical analysis. In this particular case, this analysis was conducted according to IIW guidelines [3, 27]. Experimental results exceeding a fatigue life of  $10^7$  cycles were excluded from the statistical analysis, aligning with similar practices observed for example in [28], due to the distinct change in the slope of the S-N curve observed beyond this fatigue life value. Additionally, to ensure robust statistical evaluation, data from OPB and IPB configurations with very similar geometry and loading conditions were merged into a single dataset

Figures 6, 7 and 8 present, in the form of normalized S-N curves, results from experimental fatigue life tests and numerical stress calculations. The stress data in these figures are plotted as normalized, achieved by dividing the calculated stress values by the corresponding FAT value for each specimen configuration and evaluation approach. This normalization enables effective comparison of results for different specimen configurations and loading conditions. Additionally, each graph includes the  $FAT_{norm}$  value, representing the normalized stress range at  $2 \cdot 10^6$  cycles to failure obtained from the data mean fit curve, and the scatter range index  $T_{\sigma}$ , defined according to [1] from the following equation:

$$T_{\sigma} = \frac{\sigma_{A10\%}}{\sigma_{A90\%}} \tag{5}$$

where the stress amplitudes  $\sigma_{A10\%}$  and  $\sigma_{A90\%}$  refer to the stress values corresponding to the specific number of cycles to failure with failure probabilities equal to 10% and 90%, respectively. In the case of the OPB configuration, nominal stress results were omitted from the plot due to the high ambiguity associated with the definition of this stress type in this specific specimen configuration.

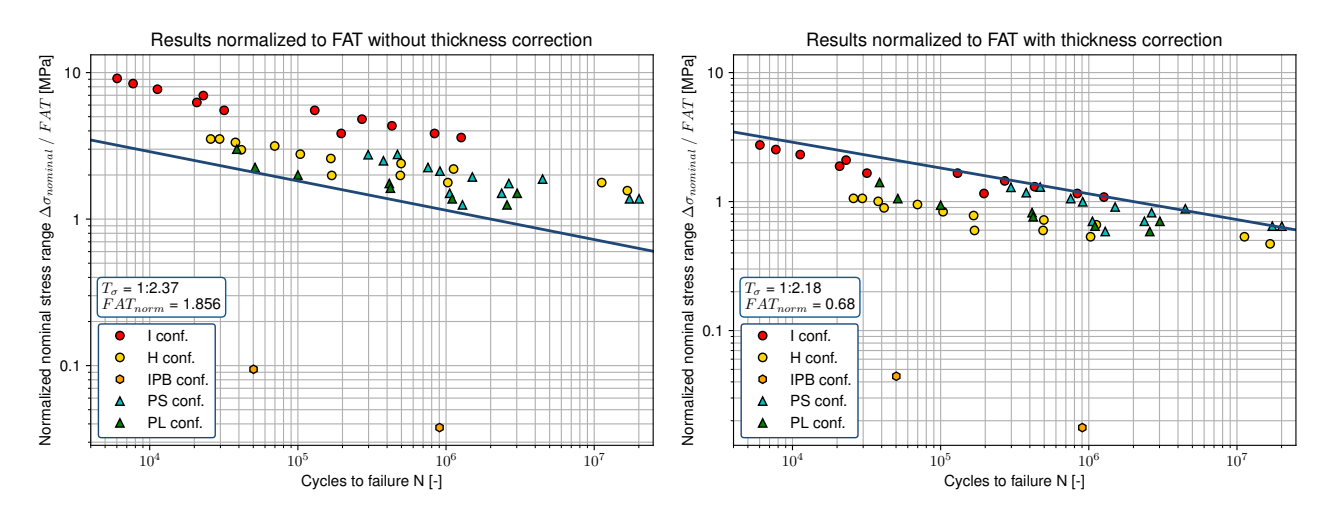


Figure 6 – Normalized S-N Curves Corresponding to the Nominal Stress Based Prediction Approach.

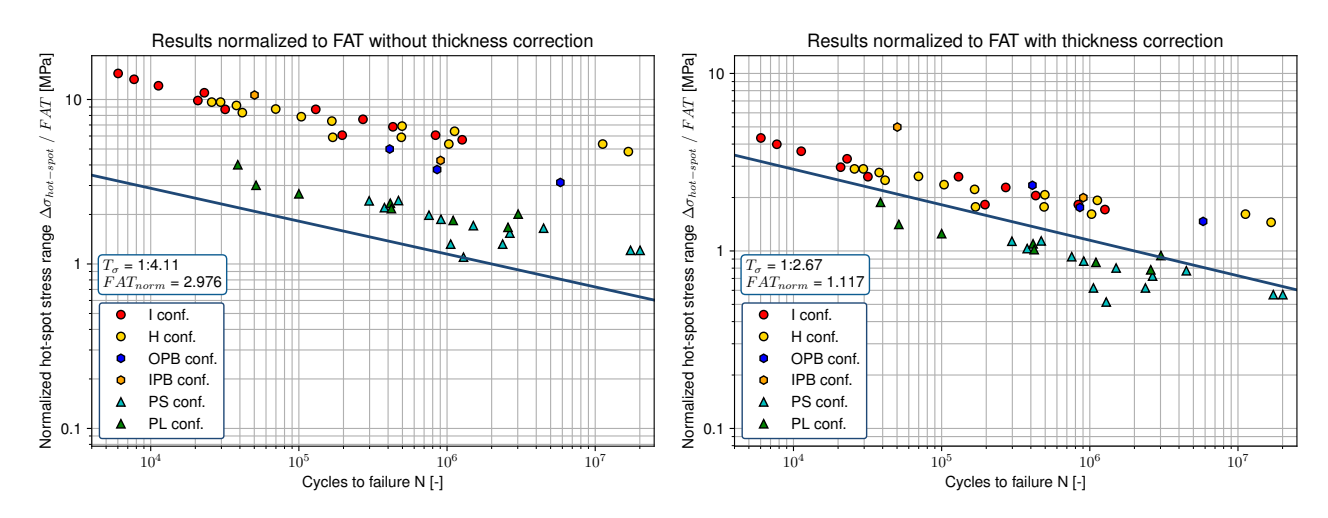


Figure 7 – Normalized S-N Curves Corresponding to the Hot-Spot Stress Based Prediction Approach.

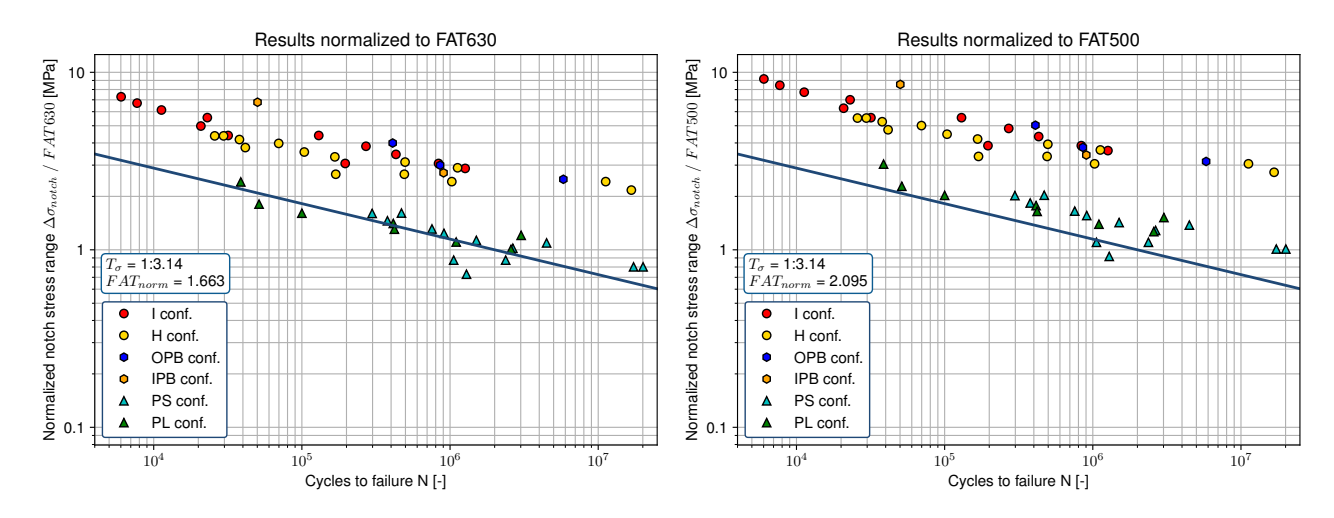


Figure 8 – Normalized S-N Curves Corresponding to the Notch Stress Based Prediction Approach.

In the case of local stress based prediction approaches (hot-spot stress based and notch stress based), a considerable split between the results is observed, leading to the formation of two parallel S-N curves. The first S-N curve includes results from the PS and PL configurations, while the

second S-N curve comprises results from the remaining specimen configurations. This split is likely caused by the different stress distributions near the critical areas of each specimen. However, further investigation is needed to confirm this assumption.

In addition to the general comparison of S-N curves, the slope of the S-N curve m for each specimen configuration was evaluated. The results are summarized in Table 4. Each slope was calculated from the notch stress values and remains constant for all other stress types, except for the H configuration. Due to the nonlinearity in loading, the m value for the H configuration slightly varies, with a lower value based on the nominal stress based prediction approach compared to the other two local approaches.

Table 4 – S-N curve slopes based on the experimental fatigue lives and calculated notch stress.

Specimen configuration:	I conf.	H conf.	OPB & IPB conf.	PS conf.	PL conf.
Mean S-N curve slope:	5.58	5.92	3.98	2.20	5.49

Table 4 shows that, except for the PS configuration, all S-N curve slopes varied between four and six, which is generally consistent with expectations and findings from other authors (e.g., [7]). The anomaly observed with the PS configuration can be attributed to specimens subjected to nominal load levels of  $100\,\mathrm{MPa}$  and  $120\,\mathrm{MPa}$ . However, as detailed in the source document [24], this behavior is likely atypical and the statistical sample is too small to accurately reflect it.

One potential verification of this theory involves extending the statistical sample by combining the results of the PS configuration with those of the most closely related specimen type, the PL configuration, and assessing the shared slope. The resulting shared slope of 4.58 generally supports the hypothesis that the anomaly is attributed to a few outlier results.

The final comparison focused on evaluating the accuracy and consistency of the prediction S-N curve provided by IIW recommendations against the prediction S-N curve compiled from experimental data. Due to the notable split between the evaluated data (see Figures 7 and 8) the comparison was conducted separately for two groups of specimen configurations.

The first group consists of the PS and PL configurations, which show significantly lower measured fatigue lives compared to the other specimen types. The second group includes the I, H, OPB, and IPB configurations. The ratio D, calculated for two fatigue life values ( $10^5$  and  $2 \cdot 10^6$  cycles), was used as the main tool for this comparison. This ratio is based on the following equation:

$$D = \frac{\Delta \sigma_{PS_{calc}}}{\Delta \sigma_{PS_{IIW}}} \tag{6}$$

where  $\Delta\sigma_{PS_{IIW}}$  represents the stress range based on the prediction S-N curve recommended by the IIW, and  $\Delta\sigma_{PS_{calc}}$  represents the stress range based on the evaluation of experimental data from each specific group of specimen configurations.

The survival probability prediction limit was calculated according to IIW guideline [3] in a similar way to the IIW prediction curves as: "values that represent 95 % survival probability (i.e. 5 % failure probability) calculated from the mean on the basis of a two-sided confidence of 75 %" from the following equation:

$$N_{PS_{calc}} = [\log_{10}(C_{PS_{50\%}}) - k \cdot Stdv] - m_{PS_{50\%}} \cdot \log_{10}(\Delta\sigma_{PS_{calc}})$$
(7)

where  $N_{PS_{calc}}$  is the predicted number of cycles,  $\log_{10}\left(C_{PS_{50\%}}\right)$  is the constant value from the mean logarithmic extrapolation of the S-N line data, Stdv is the standard deviation of the extrapolation,  $m_{PS_{50\%}}$  is the exponent of the S-N curve obtained from the extrapolation of the S-N line data, and k is the following constant:

$$k = \frac{t_{\left(\frac{0.75}{2}, n-2\right)}}{\sqrt{n}} + t_{\left(0.95, n-2\right)} \cdot \sqrt{1 + \frac{1}{n}}$$
(8)

where n is the number of experiments in each dataset and t represents the corresponding Student's t-distribution value.

The results of *D* values are presented in Tables 5, 6, 7 and 8. Values from the IPB configuration and OPB configuration were again excluded from the nominal stress based comparison due to the ambiguity in defining nominal stress in the case of the OPB configuration.

Table 5-D values calculated for  $2 \cdot 10^6$  cycles to Table 6-D values calculated for  $2 \cdot 10^6$  cycles to failture from base FAT values.

Approach	PS & PL conf.	Rest conf.
Nominal	0.829	1.073
Hot-Spot	1.049	3.022
Notch	0.695	1.573

Approach	PS & PL conf.	Rest conf.
Nominal	0.389	0.323
Hot-Spot	0.492	1.009
Notch	0.876	1.982

Table 7 - D values calculated for  $10^5$  cycles to failture from base FAT values.

Approach	PS & PL conf.	Rest conf.
Nominal	0.947	1.073
Hot-Spot	1.166	3.248
Notch	0.735	1.587

Table 8 – D values calculated for  $10^5$  cycles to failture from modified FAT values.

Approach	PS & PL conf.	Rest conf.
Nominal	0.444	0.323
Hot-Spot	0.546	1.008
Notch	0.926	1.999

Value *D* generally compares predictions based on IIW-recommended prediction S-N curves with those compiled from experimental data with the same prediction probability and should generally be higher than one. Values higher than one indicate that the prediction S-N curves recommended by IIW guidelines provide conservative results for the specific specimen configuration and prediction approach. However, excessively high values are also undesirable because they indicate overly conservative predictions. Conversely, values lower than one suggest that the prediction S-N curves recommended by IIW guidelines yield non-conservative results for the specific specimen configuration and prediction approach.

Due to the relatively small size of the statistical samples used in this evaluation compared to the size of statistical samples used to establish each IIW prediction S-N curve, sometimes even a value slightly lower than one can indicate good prediction accuracy. This is the case, for example, with the notch stress prediction of PS & PL configuration fatigue life according to FAT500 (see Figure 8).

## 5. Conclusion

This study compares three main stress-based fatigue approaches using six types of specimens. The theoretical background of each prediction approach was supplemented with practical demonstrations for defining each stress type, followed by the comparison of these fatigue life prediction approaches. From the conducted comparison of normalized stress range values, it can be concluded that among the utilized prediction approaches, the nominal stress based prediction approach exhibits the minimal scatter of results. This suggests that when the structural detail is well-known and established, this approach is a reliable prediction tool. However, for atypical geometries, such as those of the OPB and IPB configurations, this prediction approach either cannot be established or yields completely misleading results.

For the global, nominal stress-based approach, results were distributed homogeneously, with no major split between the different types of specimens. However, for the local, hot-spot, and notch stress-based approaches, a clear split can be observed between data related to the PS and PL configurations and the I, H, OPB, and IPB configurations. This observed split hindered a coherent evaluation of the data as a unified statistical set and indicates the need to investigate additional corrections that include parameters beyond wall thickness, likely related to the stress distribution near the critical area.

In the case of the nominal stress based approach, implementing thickness effect modification reduced the scatter but resulted in highly non-conservative results for all specimen types. This finding is in general agreement with the IIW guide's assumption [3] that the application of beneficial thickness correction should always be supported by component tests and must not be taken for granted.

Results without thickness effect modification even suggest that there may be no need to implement any thickness correction at all.

For the hot-spot stress based approach, using the prediction with base FAT values showed very conservative results and large scatter. The proposed thickness modification significantly reduced the scatter and worked well for the I, H, OPB, and IPB configurations but gave non-conservative results for the PS and PL configurations.

The notch stress-based approach, based on FAT630, generally provided conservative results for the I, H, OPB, and IPB configurations and non-conservative results for some PS and PL specimen configurations. The modification proposed in [21] worked very well for the PS and PL specimen configurations but gave very conservative results for the rest of the specimen configurations.

The slopes of the S-N curves generally correspond with the estimated values. The deviation in the PS configuration was caused by the anomaly of a few individual specimens, which were too large to be accurately handled within the size of this particular statistical sample.

Regarding prediction accuracy for both evaluated cycles to failure ( $10^5$  and  $2 \cdot 10^6$ ), results of the I, H, OPB, and IPB specimen configurations showed that almost all prediction approaches yield conservative or overly conservative results. Conversely, for the PS and PL specimen configurations, most prediction approaches are non-conservative.

In general, one of the best prediction approaches is based on notch stress and supplemented by the FAT values according to [21]. This prediction approach is applicable to all specimen configurations, providing almost accurate results for the PS and PL configurations, and in the case of the I, H, OPB, and IPB specimen configurations, the results are less overly conservative compared to the base hot-spot stress based prediction approach. The significant differences in prediction results between the two evaluated groups of specimen configurations again suggest the need for an additional parameter or correction to allow more accurate prediction of the fatigue life of thin-walled welded joints.

## 6. Acknowledgement

This work has been supported by the project No. FSI-S-23-8163 funded by The Ministry of Education, Youth and Sport (MEYS, MŠMT in Czech) institutional support.

The research by the authors from CTU in Prague was supported by the Grant Agency of the Czech Technical University in Prague (SGS23/156/OHK2/3T/12 project).

## 7. Contact Author Email Address

mailto: Martin.Sladky@vutbr.cz or sladkymartin97@gmail.com

### 8. Copyright Statement

The authors confirm that they, and/or their company or organization, hold copyright on all of the original material included in this paper. The authors also confirm that they have obtained permission, from the copyright holder of any third-party material included in this paper, to publish it as part of their paper. The authors confirm that they give permission, or have obtained permission from the copyright holder of this paper, for the publication and distribution of this paper as part of the ICAS proceedings or as individual off-prints from the proceedings.

### References

- [1] Radaj J, Sonsino C M and Fricke W. *Fatigue assessment of welded joints by local approaches*. First Edition, Woodhead Publishing Limited, 2006. ISBN 978-1-85573-948-2.
- [2] Gurney T R. *Cumulative damage of welded joints*. First Edition, Woodhead Publishing Limited, 2006. ISBN 978-1-85573-938-3.
- [3] Hobbacher A F. *Recommendations for Fatigue Design of Welded Joints and Components*. Second Edition, Springer Cham, 2016. https://doi.org/10.1007/978-3-319-23757-2.
- [4] Niemi E, Fricke W. and Maddox S J. *Structural Hot-Spot Stress Approach to Fatigue Analysis of Welded Components*. Second Edition, Springer Singapore, 2018. https://doi.org/10.1007/978-981-10-5568-3.
- [5] Fricke W. *IIW Recommendations for the Fatigue Assessment of Welded Structures by Notch Stress Analysis*. First Edition, Woodhead Publishing Limited, 2012. https://doi.org/10.1533/9780857098566.
- [6] Kang G and Luo H. Review on fatigue life prediction models of welded joint. *Acta Mechanica Sinica*, Vol. 36, pp 701–726, 2020. https://doi.org/10.1007/s10409-020-00957-0.
- [7] Sonsino C M, Bruder T and J Baumgartner. S-N Lines for Welded Thin Joints Suggested Slopes and FAT Values for Applying the Notch Stress Concept with Various Reference Radii. *Welding in the World*, Vol. 54, pp 375-392, 2010. https://doi.org/10.1007/BF03266752.
- [8] Macdonald K A. *Fracture and fatigue of welded joints and structures*. First Edition, Woodhead Publishing Limited, 2011. ISBN 978-1-84569-513-2.
- [9] European Committee for Standardization (CEN). EN 1993-1-9, Eurocode 3: Design of steel structures Part 1-9: Fatigue. 2005.
- [10] British Standards Institution (BSI). BS 7608, Guide to fatigue design and assessment of steel products. 2014.
- [11] European Convention for Constructional Steelwork (ECCS). *ECCS 43, Recommendations for the fatigue design of steel structures.* 1985.
- [12] Deutscher Verband für Schweißen und verwandte Verfahren (DVS). DVS 0905, Industrielle Anwendung des Kerbspannungskonzept Es für den Ermüdungsfestigkeitsnachweis von Schweißverbindungen. 2017.
- [13] Zhao X-L, Herion S, Packer J A, Puthli R S, Sedlacek G et al. *Fatigue Design Procedure for Welded Hollow Section Joints*. 1st edition, Woodhead Publishing Limited, 2000. ISBN 978-1-85573-522-4
- [14] Dong P. A structural stress definition and numerical implementation for fatigue analysis of welded joints. *International Journal of Fatigue*, Vol. 23, 865-876, 2001. https://doi.org/10.1016/S0142-1123(01)00055-X.
- [15] Xiao Z G and Yamada K. A method of determining geometric stress for fatigue strength evaluation of steel welded joints. *International Journal of Fatigue*, Vol. 26, 1277-1293, 2004. https://doi.org/10.1016/j.ijfatigue.2004.05.001.
- [16] Neuber H. *Theory of Notch Stresses: Principles for Exact Stress Calculation*. First Edition, J.W. Edwards, 1946. ISBN 978-0-59897-257-6.
- [17] Radaj D, Lazzarin P and Berto F. Generalised Neuber concept of fictitious notch rounding. *International Journal of Fatigue*, Vol. 51, 105-115, 2013. https://doi.org/10.1016/j.ijfatigue.2013.01.005.
- [18] Fischer C, Fricke W and Rizzo C M. Experiences and recommendations for numerical analyses of notch stress intensity factor and averaged strain energy density. *Engineering Fracture Mechanics*, Vol. 165, 98–113, 2016. https://doi.org/10.1016/j.engfracmech.2016.08.012.
- [19] Zhang G and Richter B. A new approach to the numerical fatigue-life prediction of spot-welded structures. *Fatigue & Fracture of Engineering Materials & Structures*, Vol. 23, 499–508, 2000. https://doi.org/10.1046/j.1460-2695.2000.00316.x.
- [20] Baumgartner J. Review and considerations on the fatigue assessment of welded joints using reference radii. *International Journal of Fatigue*, Vol. 101, 459-468, 2017. https://doi.org/10.1016/j.ijfatigue.2017.01.013.
- [21] Baumgartner J, Hobbacher A F and Rennert R. Fatigue assessment of welded thin sheets with the notch stress approach Proposal for recommendations. *International Journal of Fatigue*, Vol. 140, 1-14, 2020. https://doi.org/10.1016/j.ijfatigue.2020.105844.
- [22] Fricke W, Paetzold H and Zipfel B. Fatigue Tests and Numerical Analyses of a Connection of Steel Sandwich Plates. *Welding in the World*, Vol. 53, 151–157, 2009. https://doi.org/10.1007/BF03266726.
- [23] Machač M, Papuga J, Doubrava K and Fišer J. Fatigue Analysis of Thin-Walled Welded Hollow Section Joints. *Fatigue and Fracture of Materials and Structures*, Wrocław (Poland) and remote form, Vol. 24, 6, pp 49-55, 2022. https://doi.org/10.1007/978-3-030-97822-8 6.
- [24] Gurney T R. Fatigue of thin walled joints under complex loading. First Edition, Woodhead Publishing Limited, 1997. ISBN 978-1-85573-338-1.

- [25] Cormier N G, Smallwood B S, Sinclair G B and Meda G. Aggressive submodelling of stress concentrations. *International Journal for Numerical Methods in Engineering*, Vol. 46, pp 889-909, 1999. https://doi.org/10.1002/(SICI)1097-0207(19991030)46:6<889::AID-NME699>3.0. CO;2-F.
- [26] Baumgartner J and Bruder T. An efficient meshing approach for the calculation of notch stresses. *Welding in the World*, Vol. 57, pp 137–145, 2013. https://doi.org/10.1007/s40194-012-0005-3.
- [27] Parmentier G, Huther M, Huther I and Lefebvre F. Best Practice Guideline for Statistical Analyses of Fatigue Results. 1st edition, Springer Cham, 2023. https://doi.org/10.1007/978-3-031-23570-2.
- [28] Bruder T, Störzel K, Baumgartner J and Hanselka H. Evaluation of nominal and local stress based approaches for the fatigue assessment of seam welds. *International Journal of Fatigue*, Vol. 34, pp 86-102, 2012. https://doi.org/10.1016/j.ijfatigue.2011.06.002.